Received: 14 March 2017 | Accepted: 18 May 2018

DOI: 10.1111/pce.13354

ORIGINAL ARTICLE

WILEY Plant, Cell & Environment

FITNESS, a CCT domain-containing protein, deregulates reactive oxygen species levels and leads to fine-tuning trade-offs between reproductive success and defence responses in Arabidopsis

Ana Virginia Osella[1]* | Diego Alberto Mengarelli[1]* | Julieta Mateos[2] | Shuchao Dong[3] | Marcelo J. Yanovsky[2] | Salma Balazadeh[3] | Estela Marta Valle[1] | María Inés Zanor[1]

[1] Instituto de Biología Molecular y Celular de Rosario (IBR-CONICET) Ocampo y Esmeralda PREDIO CCT-Facultad de Ciencias Bioquímicas y Farmacéuticas (UNR), Rosario, Argentina

[2] Fundación Instituto Leloir, Instituto de Investigaciones Bioquímicas de Buenos Aires–CONICET, Buenos Aires, Argentina

[3] Max-Planck Institute of Molecular Plant Physiology, Potsdam, Germany

Correspondence
María Inés Zanor, Instituto de Biología Molecular y Celular de Rosario (IBR-CONICET) Ocampo y Esmeralda PREDIO CCT-Facultad de Ciencias Bioquímicas y Farmacéuticas (UNR) Suipacha 531-2000 Rosario, Argentina.
Email: zanor@ibr-conicet.gov.ar

Funding information
Bayer Science & Education Foundation, Grant/Award Number: F-2016-JS-0261; CONICET, Grant/Award Number: PIP-236; ANPCYT, Grant/Award Number: PICT-2012-2709

Abstract

Environmental stresses are the major factors that limit productivity in plants. Here, we report on the function of an uncharacterized gene *At1g07050*, encoding a CCT domain-containing protein, from *Arabidopsis thaliana*. *At1g07050* expression is highly repressed by oxidative stress. We used metabolomics, biochemical, and genomic approaches to analyse performance of transgenic lines with altered expression of *At1g07050* under normal and oxidative stress conditions. *At1g07050* overexpressing lines showed increased levels of reactive oxygen species (ROS), whereas knock-out mutants exhibited decreased levels of ROS and higher tolerance to oxidative stress generated in the chloroplast. Our results uncover a role for *At1g07050* in cellular redox homeostasis controlling H_2O_2 levels, due to changes in enzymes, metabolites, and transcripts related to ROS detoxification. Therefore, we call this gene *FITNESS*. Additionally, several genes such as *ACD6*, *PCC1*, and *ICS1* related to salicylic acid signalling and defence were found differentially expressed among the lines. Notably, FITNESS absence significantly improved seed yield suggesting an effective fine-tuning trade-off between reproductive success and defence responses.

KEYWORDS

cell death, flowering time, metabolism, oxidative stress, photorespiration, seed yield

1 | INTRODUCTION

Plant growth is limited by adverse environmental conditions. Environmental stresses can suppress light utilization and induce aberrant electron flow in chloroplasts. The consequence of this is an increase of reactive oxygen species (ROS) levels due to partial reduction of oxygen molecules (Mittler, Vanderauwera, Gollery, & Van Breusegem, 2004) leading to cell oxidative stress. Production of ROS during environmental stress in plants is one of the main causes for injury, death, and decreases in productivity. Plant cells respond to oxidative stress by removing the produced ROS. Therefore, the type of ROS that accumulates in the cells is determined by a subtle balance between ROS producing and scavenging activities. The ROS scavenging system includes low molecular mass components (ascorbic acid, reduced glutathione, and tocopherols) and antioxidant enzymes such as superoxide dismutase (SOD), catalase (CAT), ascorbate peroxidase (APX), glutathione peroxidase, and glutathione reductase (GR; Mittler et al., 2004). In photosynthetic tissues, the main sources of ROS are the chloroplasts and peroxisomes, and its formation is related to the

*Ana Virginia Osella and Diego Alberto Mengarelli contributed equally to this work and should both be considered first authors.

photosynthetic and photorespiratory processes. Plants trigger the early expression of different sets of genes involved in antioxidant signalling pathways and transcriptional regulation to cope with the daily, unavoidable, oxidative condition (Baxter, Mittler, & Suzuki, 2013). The mechanisms involved in the coordination of the activated signals at different times and places are still unclear.

Previous investigations (Scarpeci, Zanor, Carrillo, Mueller-Roeber, & Valle, 2008) had shown that a rapid response of *Arabidopsis thaliana* leaves to chloroplast-generated ROS included a strong up-regulation of genes involved in abiotic stress responses and transcription and down-regulation of few genes most of them encoding proteins with unknown functions. One of the latter genes (*At1g07050*) encodes a hypothetical protein similar to one of rice (*Hd1*, a homologue of *CONSTANS* from Arabidopsis) involved in the photoperiod sensitivity (Yano et al., 2000). It is known that the duration of the day length influences the generation of ROS (Michelet & Krieger-Liszkay, 2012) and it is a critical determinant of the oxidative stress response (Queval et al., 2007). In Arabidopis, the transcription factor CONSTANS (CO) promotes flowering under long day (Puterill, Robson, Lee, Simon, & Coupland, 1995), and in barley, it controls floral repression by up-regulating *VERNALIZATION2* (Mulki & von Korff, 2016). *CO* is circadian regulated, and its degradation is light-induced. CO belongs to a larger family called CONSTANS LIKE (COL), which encodes proteins with a conserved region present in the carboxy-terminus, termed the CCT (CO, COL, and TIMING OF CAB EXPRESSION1) domain in addition to a zinc finger region that resembles a B-box domain present in the amino-terminus, which regulates protein–protein interactions. The CCT domain can directly bind to DNA, and CCT-containing proteins act as transcription factors (Gendron et al., 2012; Tiwari et al., 2010). Genes encoding CCT domain proteins have been implicated in processes such as photoperiodic flowering (Puterill et al., 1995), light signalling (Kaczorowski & Quail, 2003), and regulation of circadian rhythms (Strayer et al., 2000) and plant architecture (Ordoñez Herrera et al., 2018). In recent investigations, the CCT domain was included in a larger family of uncharacterized genes which possess a single CCT domain called *CCT MOTIF FAMILY* genes (Cockram et al., 2012). They are present in monocot and dicot plant species. In Arabidopsis, the family comprises 15 members, and despite significant progress in recent years, the function of the vast majority of them still remains enigmatic. The control of flowering time is a crucial environmental adaptation in plants, as well a major determinant of seed yield. Environmental and endogenous signals determine via intricate molecular pathways flowering time, and the major cues for floral transition are seasonal changes in photoperiod (Cockram et al., 2012). Here, we report about the role of the uncharacterized gene *At1g07050*, encoding a protein with a single CCT domain. This domain is a conserved region which mediates DNA binding. We observed that knock-out plants exhibited decreased levels of ROS and higher tolerance to oxidative stress. Additionally, these mutants accumulated higher levels of salicylic acid (SA) and showed increased seed production. On the contrary, *At1g07050* overexpressing plants accumulated high levels of ROS being its clearance capability overwhelmed. We postulate that *At1g07050* acts as a link between stress-activated responses and developmental programs which are crucial to obtain a good yield, and therefore we called this gene *FITNESS*.

2 | MATERIAL AND METHODS

2.1 | General

DNA sequencing was performed by the University of Maine DNA sequencing facility (USA, Orono, ME). For sequence analyses, the tools provided by the National Center for Biotechnology Information (http://www.ncbi.nlm.nih.gov/), the Arabidopsis Information Resource (TAIR; http://www.arabidopsis.org/), and WolF Sort (http://www.genscript.com/wolf-psort.html) were used. Chemicals and reagents were obtained from Sigma-Aldrich (St Louis, USA) or Merck (Buenos Aires, Argentina). Restriction enzymes and reagents for quantitative PCR (qPCR) were provided by Promega and Invitrogen Life Technologies (Buenos Aires, Argentina).

2.2 | Constructs and plants

Constructs were generated by PCR- and restriction enzyme-mediated cloning. Primer sequences are given in Table S1. PCR-generated amplicons were checked by DNA sequence analysis. Constructs were transformed into *A. thaliana* (L.) Heynh. cv. Col-0 via *Agrobacterium*-mediated transformation. *Agrobacterium tumefaciens* strain GV3101pmp90 and GV3101 pSOUP were used for plant transformation. *Arabidopsis* individual plants were grown in controlled growth chambers in 6-cm pots at approximately 70% relative humidity with a 16-hr light/8-hr dark period for long day conditions (23°C, 120 μmol m^{-2} s^{-1}). The T-DNA insertion line (*fitness-1* mutant SALK_140249) was obtained from the Arabidopsis Biological Resource Center, The Ohio State University. Homozygous plants were identified by PCR using the T-DNA left border and the gene-specific RP primers. Site-directed mutagenesis in *A. thaliana* using dividing tissue-targeted RGEN of the CRISPR/Cas system to generate heritable null alleles mutated via CRISPR/Cas9 technology as described in Hyun, Cho, Choi, Kim, and Coupland (2015) was used to obtain a second *fitness* mutant (*fitness-2*). Target sequence was directed to the first exon. U6p::sgRNA cassette was generated by overlapping PCR using AT1G07050-A1 and Sg1 primers for PCR1 and AT1G07050-A2 and Sg2 primers for PCR2. A second PCR was performed using Sg1 and Sg2 primers and both fragments. The fragment was cloned into pYB196 binary vector and used to transform Agrobacterium GV3011 with pSOUP. Arabidopsis plants transformed via floral dip were selected in soil with BASTA. T1 transgenic lines were selected by the polymorphism test using T7E1 endonuclease assay and sequencing.

$FITNESS_{ox}$: *At1g07050* open reading frame was amplified by PCR from Arabidopsis Col-0 seedling cDNA and inserted into pCR-Blunt using primers FITNESS_fw and FITNESS_rev. The cDNA was cloned downstream of the cauliflower mosaic virus (CaMV) 35S promoter into the binary expression vector pBinAR as in Scarpeci, Zanor, Mueller-Roeber, and Valle (2013).

FITNESS:GFP: for stable expression of FITNESS:GFP (green fluorescence protein) fusion protein in Arabidopsis plants, the *At1g07050* coding region was PCR amplified from Arabidopsis Col-0 seedling cDNA using primers FITNESS_fw and FITNESS_rev (without stop) and then

inserted into pCR Blunt vector. The cDNA was cloned downstream of the CaMV 35S promoter into the binary expression vector pCHF3 (Jarvis et al., 1998).

promFITNESS::GUS fusion: the full intergenic genomic fragment upstream of the translation initiation codon of *At1g07050* (383 bp) was amplified by PCR from Arabidopsis Col-0 genomic DNA using primers FITNESS_prom_fw and FITNESS_prom_rev and inserted into plasmid pCR-Blunt. The promoter fragment was cloned into pBI101.1 as previously described (Scarpeci et al., 2008).

To perform all the experiments, we grew all plants alongside each other under carefully controlled conditions. All experiments were repeated at least three times.

2.3 | RNA-seq transcriptome analysis

For each genotype, three biological replicates were analysed, consisting of a pool of 20 two-weeks old seedlings. Total RNA was extracted using RNeasy Plant Mini Kit (Qiagen). RNAseq libraries and sequencing were performed by BGI TECH SOLUTIONS (HONGKONG) CO. Limited. rRNA was removed using oligo (dT) magnetic beads. Libraries were prepared according to the protocol (Illumina). The same amount of each RNAseq library was run on one lane of HiSeqTM 4000 (Illumina), with the read desired length of 50 pb. The quality of the sequencing reads was assessed with FASTQC (http://www.bioinformatics.babraham.ac.uk/projects/fastqc/). RNA sequencing reads were trimmed using DynamicTrim (Phred score $\geq$ 20). RNAseq reads were aligned against the *A. thaliana* transcriptome (Pertea, Kim, Pertea, Leek, & Salzberg, 2016) using hisat2 v2.1.0 (Kim, Langmead, & Salzberg, 2015), generated raw read counts for each transcript. DESeq v1.31.0 (Anders & Huber, 2010) was used to run two differential expression analysis tests: between WT and *fitness* and between WT and *OX-1*. For Gene Ontology (GO) enrichment analysis, the agriGO v2.0 platform was used (Tian et al., 2017).

2.4 | ROS staining procedures

H_2O_2 and superoxide anion were detected as previously described (Scarpeci et al., 2008). To quantify the formazan produced after NBT reduction in histochemical staining of leaves, a described procedure was used (Bournonville & Díaz-Ricci, 2011).

2.5 | Quantitative PCR

Total RNA was prepared using TRIzol (Invitrogen Life Technologies) following the manufacturer's procedure. RNA quality and quantity, as well as RNA reverse transcription and qPCR, were performed as previously described (Scarpeci et al., 2013). Primer sequences are given in Table S1. PCR reactions were carried out in a Mastercycler ep Realplex thermocycler (Eppendorf, Westbury, USA) using a SYBR Green fluorescence-based assay. The relative expression ratio for each gene was calculated as previously described (Pfaffl, 2001). The PCR efficiency for each reaction was calculated based on the profile of the emitted fluorescence in the exponential phase (Rutledge & Stewart, 2008). Normalization was done according to Czechowski, Stitt, Altmann, Udvardi, and Scheible (2005) determining the transcripts levels of *PROTEIN PHOSPHATASE 2a* (*PP2a*, *At1g13320*) gene.

2.6 | Chlorophyll and free proline content

Twenty milligrams fresh weight (FW) plant material were extracted twice with 80% ethanol (Merck)/10 mM MES (pH 5.9; Sigma-Aldrich) and once with 50% Ethanol/10 mM MES (pH 5.9). Ethanolic extracts were mixed and used for chlorophyll and free Proline (Pro) content determination in a polystyrene 96-deep well plate as in Scarpeci, Frea, Zanor, and Valle (2017).

2.7 | Metabolite profiling by gas chromatography coupled to mass spectrometry

Metabolite extraction was performed using 100 mg FW of ground leaf material collected at noon. Extraction, derivatization, and relative metabolite levels were determined using an established gas chromatography coupled to mass spectrometry protocol as described previously (Lisec, Schauer, Kopka, Willmitzer, & Fernie, 2006). Metabolites were identified in comparison with database entries of authentic standards (Schauer et al., 2005).

2.8 | Glyoxylate

Glyoxylate measurement was conducted using the protocol described by Häusler, Bailey, Lea, and Leegood (1996).

2.9 | Chlorophyll fluorescence

Arabidopsis plants were dark-adapted for 30 min before measurements. Chlorophyll fluorescence was measured at 23°C employing a Dual PAM-100 (Walz GmbH, Germany).

2.10 | Extraction and assay of enzyme activities

Aliquots of 20 mg FW of ground plant material were used for APX, CAT, and GR activities assays, as previously described (Scarpeci et al., 2008). SOD in-gel activity was determined as previously described (Beauchamp & Fridovich, 1971).

2.11 | Methyl viologen treatment of plants

Plants grown on soil under normal conditions were sprayed with 15 or 50 μM methyl viologen (MV), 0.01% (*v*/*v*) Tween 20. Control plants grown in parallel were handled as treated plants except that MV was omitted. At 2 hr after treatment, one leaf per plant was separated to assay for superoxide presence using NBT staining. Survival of the plants after the treatment was monitored during 2 weeks.

2.12 | Phylogenetic analysis

AtCMF protein sequences (Table S2) were aligned using ClustalW, and phylogenetic analysis was conducted on the resulting alignments using ClustalX2.1 (Larkin et al., 2007). The phylogenetic tree was inferred

using the neighbour-joining method. Unrooted phylogenies were determined using the distance matrix method, with tree topographies supported by bootstrapping (1,000 replicates). For tree visualization, we used TreeView 1.6.6 (Page, 1996). The scale bar means 0.1 nucleotide substitutions/site.

2.13 | Microscopy and hystochemical staining

Distribution of FITNESS:GFP fusion protein was analysed by confocal fluorescence microscopy using an Eclipse TE 2000-E2 microscope (Nikon, Düsseldorf, Germany). GUS assay was performed essentially as in Scarpeci et al. (2008). Trypan Blue staining was performed as in Rusterucci, Aviv, Holt, Dangl, and Parker (2001).

2.14 | Statistical analyses

Statistical analyses were performed using the *t* test embedded in the Microsoft Excel software. Only the return of $P < 0.05$ was designated statistically significant. $P < 0.05$ is indicated by *. For one-way analysis of variance followed by Fisher's least significant difference multiple comparison test, InfoStat 2008 for Windows was used (Di Rienzo et al., 2008).

3 | RESULTS

3.1 | Phenotypic effects of altered *FITNESS* expression in Arabidopsis lines

FITNESS was found differentially expressed in Arabidopsis plants after treatment with MV, a $O_2^{\cdot-}$ inducer in the light resulting in more than sixfold repression (Scarpeci et al., 2008). To investigate the functional role of *FITNESS* in Arabidopsis, two homozygous knock-out plants were obtained, *fitness-1*, identified from a T-DNA insertional mutant line (Figure S1a,b), and *fitness-2*, which was obtained using CRISPR/Cas9 technology by using PCR and Sanger sequencing (Figure S1a,c). The mutated sequence leads to amino acid substitution and premature stop codon formation. In addition, multiple transgenic lines overexpressing *FITNESS* under the control of the CaMV 35S promoter (*FITNESS$_{ox}$*) were generated. Three homozygous T3 independent transgenic lines (from more than 20), *FITNESS$_{ox1}$*, *FITNESS$_{ox2}$*, and *FITNESS$_{ox3}$* (Figure S1d) were selected for this work, and we chose *FITNESS$_{ox1}$* for subsequent analysis. Finally, we used the *35S:FITNESS* construct to complement *fitness-1* mutants. Quantitative PCR confirmed lower or higher *FITNESS* transcript levels in all the selected lines compared with WT plants (Figure 1a).

In addition, *FITNESS$_{ox}$* lines showed several morphological alterations, such as pale green colour, reduced size, rounded up-curled leaves which develop spontaneous lesions in their borders (Figure 1 b,c,d). On the contrary, *fitness* mutants were almost indistinguishable from WT plants; however, at later stages of development, *fitness* mutant leaves appeared slightly narrower than control plants due to downward curling of their borders (Figure 1d). Although *fitness* mutants showed no differences in flowering time compared with WT plants, *FITNESS$_{ox}$* lines started to flower in average 3 days later. We also analysed seed yield; *fitness* mutants produced a significantly higher amount of seeds per plant being the production of *FITNESS$_{ox}$* lines lower than the WT (Figure 1e).

The observation that *fitness* mutants have a higher seed yield compared with WT plants prompted us to analyse the photosynthetic parameters of these lines. To verify the integrity and functionality of PSII, several parameters associated with chlorophyll *a* fluorescence were measured (Baker & Rosenqvist, 2004). In 37-day-old plants, the photosynthetic parameters such as *Fv/Fm*, ϕPSII, and qP were similar in all the lines (data not shown), indicating that the linear electron transport rate was not altered. However, nonphotochemical quenching (NPQ) which indicates the energy fraction dissipated as heat was significantly decreased in *fitness-1 and fitness-2* mutants (Figure 1f). The same behaviour was seen in 45-day-old plants and additionally *FITNESS$_{ox}$* lines showed significantly increased NPQ when compared with WT plants (Figure S1d).

3.2 | *FITNESS* belongs to a large family of uncharacterized genes that possess just a single CCT domain

FITNESS encodes a protein of 195 amino acids (23.3 kDa) and pI 4.7, with a single CCT domain, and belongs to the CCT motif family genes. The 44 amino acids long CCT domain present in FITNESS (AtCMF3) is located between Arg-151 and Glu-194 (Figure S2a). FITNESS closest Arabidopsis homologue is the 339 amino acid protein $AtCMF_{11}$ (At5g14370; Figure S2b) with which it shares 49% identity. So far, the only member of this family whose function was previously reported is $AtCMF_{14}$ (At1g57180) also named CIA_2, which acts as a transcription factor (Sun, Huang, & Chang, 2009). Computational analysis with WoLF PSORT (Horton et al., 2007) to predict the potential subcellular localization of FITNESS anticipates nuclear localization. Therefore, the subcellular localization of FITNESS was tested by stable expression in Arabidopsis, using GFP as marker under the control of the CaMV 35S promoter. Figure 2a demonstrates that FITNESS:GFP fusion protein (~50 kDa) predominantly accumulates in the nuclear compartment of the cells, whereas free GFP typically localizes to the cytoplasm and the nucleus. To search for nuclear localization signal in FITNESS, bioinformatic analysis of the protein sequence revealed potential monopartite class 2 nuclear localization signals within the second half of the CCT domain at amino acid positions 169–172 (KKIR) and 182–185 (KRPR; Figure S2a) which resemble the consensus sequence K (K/R) X (K/R; Kosugi et al., 2009).

3.3 | Expression patterns of *FITNESS* in Arabidopsis

Arabidopsis transgenic lines harbouring the transcriptional fusion *promFITNESS::GUS* were analysed. The putative promoter sequence selected was the longest region (~383 bp) before the beginning of the following gene, and we expected that this region would be informative to monitor *FITNESS* expression "*in planta*." More than 15 independent *promFITNESS::GUS* transformants were selected and tested for GUS activity. Our analysis revealed high GUS staining in cotyledons (Figure 2bI). Seedlings of *promFITNESS::GUS* lines were analysed, and although GUS staining was high in cotyledons, a lower expression was seen in the developing true leaves (Figure 2bI,II) and fully

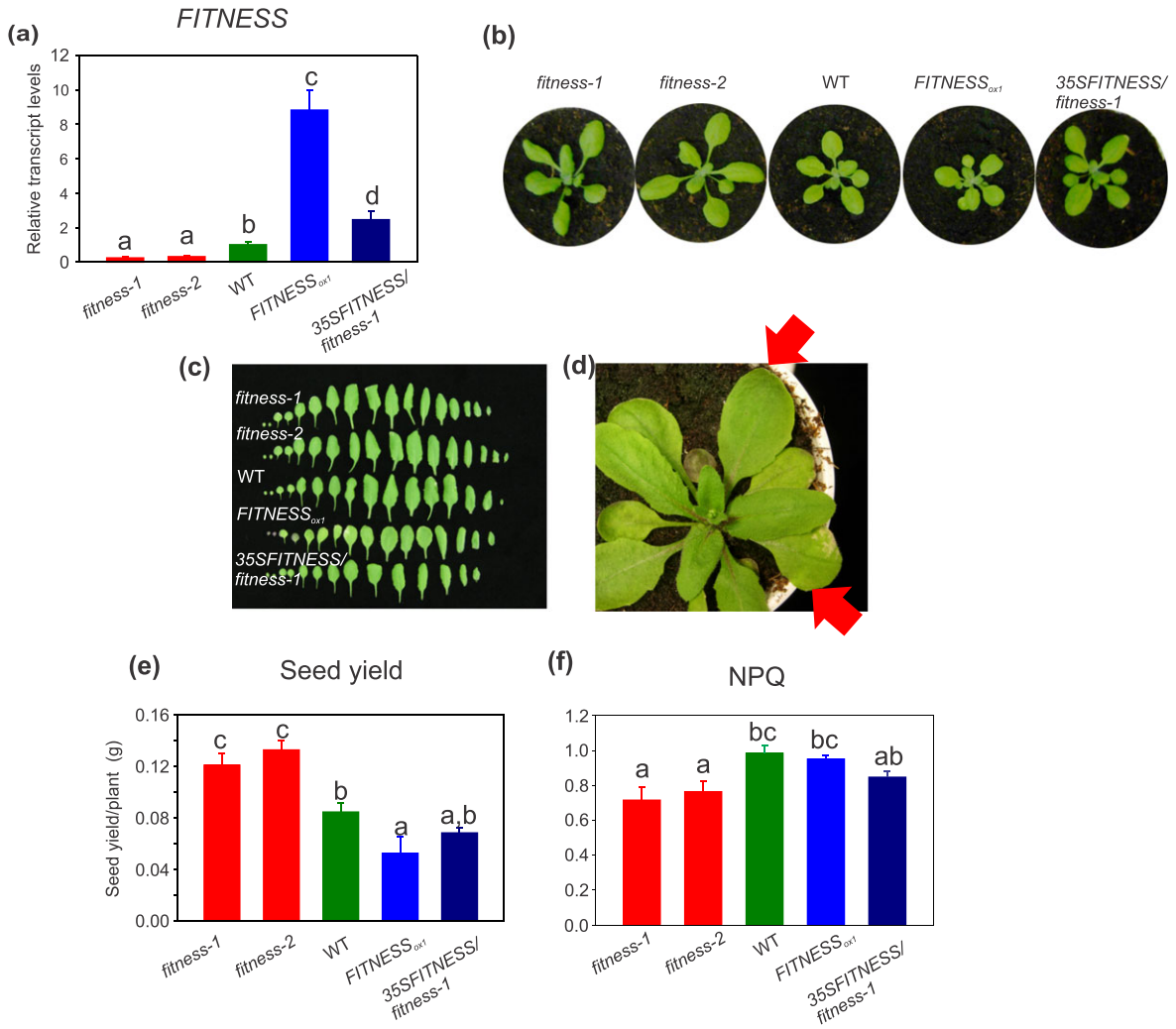

FIGURE 1 Molecular and phenotypic characterization of *FITNESS* lines. (a) *FITNESS* transcripts expression level in the selected lines. qPCR was performed on leaf material obtained from 5-week-old plants grown under long-day conditions. (b) $FITNESS_{ox}$ lines develop smaller rosette in comparison with control lines and *fitness* mutants as seen in 3-week-old representative plants. (c) Leaf series were created by dissecting 4-week-old rosettes and arranging the individual leaves. The picture includes lines with altered levels of *FITNESS* and WT. (d) Red arrows indicates spontaneous lesions in leaf border and a hyponastic leaf of a 5-week-old $FITNESS_{ox1}$ line. (e) Seed yield (in grams) per plant ($n \geq 5$). (f) Nonphotochemical quenching (NPQ) of 37 days-old plants, fluorescence was measured in attached Arabidopsis leaves, and NPQ was calculated ($n \geq 4$). Results of a representative experiment are presented as mean ± SE of biological replicates. Bars with the same letter are not significantly different from one another (analysis of variance + Fisher least significant difference, $P < 0.05$)

expanded leaves (Figure 2bIII,IV). The vascular regions of the leaves did not show GUS staining, and also, no staining was seen in the root at any developmental point (Figure 2bI–III). In older plants, *promFITNESS::GUS* expression in leaves was generally weak showing a lack of expression towards the tip. *promFITNESS::GUS* expression was also seen in sepals of floral buds (Figure 2bV) but not in siliques (Figure 2bVI). These results are in agreement with expression data retrieved from GENEVESTIGATOR (https://genevestigator.com/) and the Arabidopsis eFP Browser 2.0 (http://bar.utoronto.ca/efp2/Arabidopsis/Arabidopsis_eFPBrowser2.html).

3.4 | Transcriptional profile of *FITNESS* lines

To identify genes present in *FITNESS* transcriptomic network, we performed genome-wide transcriptome studies. Using an adjusted *P* value < 0.00001 to define differential expression, we identified 2,195 and 615 unique genes up- and down-regulated in *fitness-1* and $FITNESS_{ox1}$ lines, respectively, compared each with WT (Table S3). We performed a GO enrichment analysis on the identified differentially expressed genes, and among the most significantly GO terms are response to abiotic stimulus (GO:0009628), response to oxygen-containing compound (GO:1901700), and response to stress (GO:0006950, Figure S3a,b, and Table S5). We also searched for genes exhibiting opposed expression in mutant and overexpressor lines, and a total of 99 show this opposite expression pattern (adjusted *P* value < 0.05, Figure 3, Table S4). The GO enrichment of the differentially expressed genes exhibiting opposed expression and false discovery rate (FDR) < 0.005 include response to stimulus (GO:0050896), response to acid chemical (GO:0001101), response to oxygen-containing compound (GO:1901700), response to stress

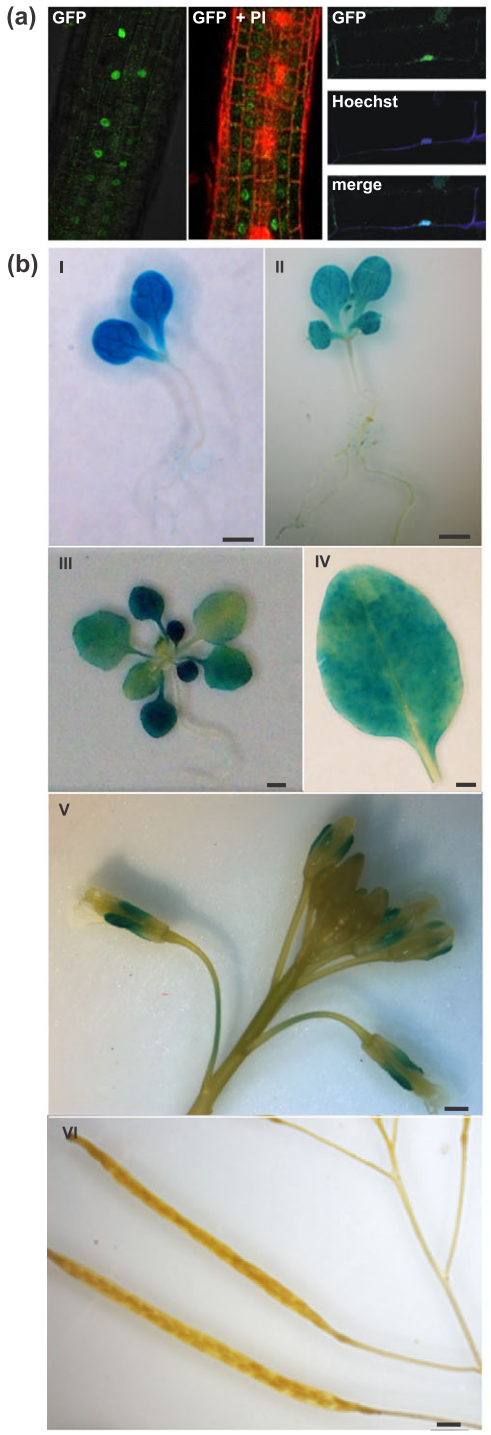

FIGURE 2 Subcellular localization of FITNESS and spatial expression pattern of *prom FITNESS:GUS*. (a) FITNESS protein subcellular localization. The *35S::FITNESS-GFP* construct was expressed in Arabidopsis plants using stable transformation. GFP subcellular localization was monitored by confocal microscopy of transformed roots. FITNESS-GFP fusion protein was exclusively localized in the nucleus (left panel), red fluorescence of propidium iodide (PI) was monitored separately (middle panel). To confirm nuclear localization, blue fluorescence of HOECHST was merged to the FITNESS-GFP fluorescence (right panel). (b) *FITNESS* promoter region was used to drive *GUS* expression in transgenic plants (*promFITNESS::GUS* lines). I: 5-day-old seedling. II: 9-day-old seedling. III: 2-week-old seedling. IV: detached leaf of 4-week-old rosette. V: flower of a 5-week-old plant. VI: siliques of 7-week-old plant. Scale bars = 1 mm (I and II); 2 mm (III, IV, V, and VI)

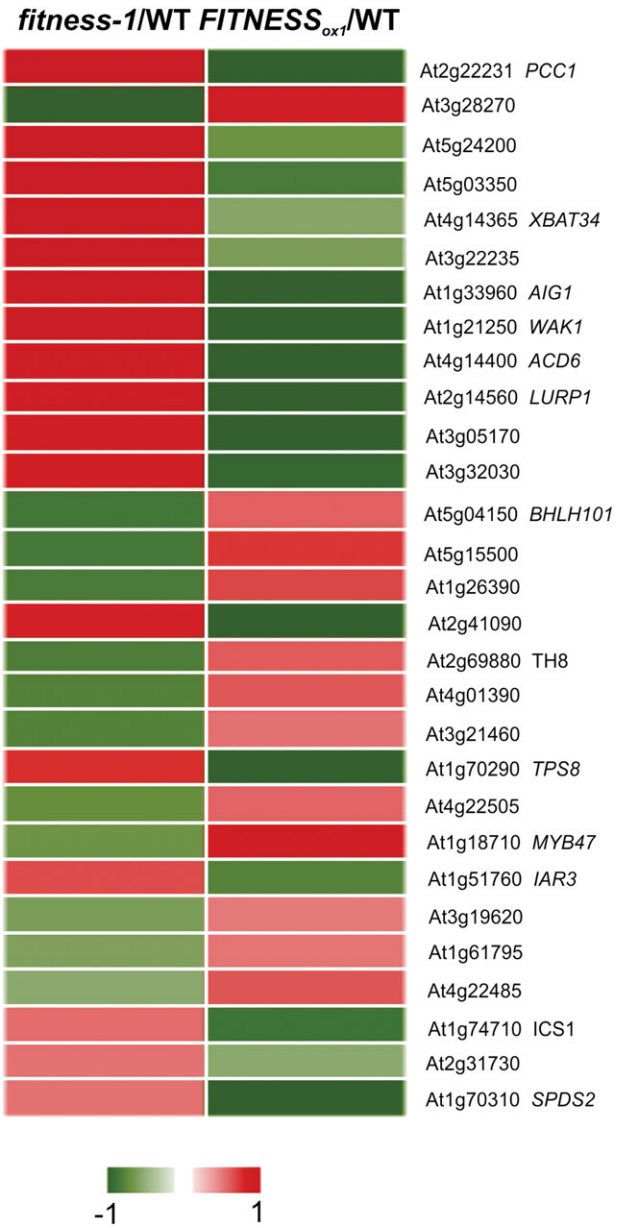

FIGURE 3 Transcript profile analysis of *FITNESS* lines. Heat map of a subset (Log2 Fold Change >0.5 and <−0.5) of differentially and opposite expressed genes between *fitness-1* and $FITNESS_{ox}$ line (see also Table S4). Green and red indicates a decrease and increase, respectively, of expression with respect to the average of the WT level. Data are expressed as log2 values (n = 3)

(GO:0006950), response to abiotic stimulus (GO:0009628), response to bacterium (GO:0009617), response to external biotic stimulus (GO:0043207), response to lipid (GO:0033993), and response to SA (SA, GO:0009751). Several genes related to SA signalling (*ACCELERATED CELL DEATH 6*, *ACD6*, *At4g14400*; *LURP1*, *At2g14560*; and *ICS1*; *At1g74710*) showed increased expression in *fitness* mutants and decreased expression in $FITNESS_{ox1}$ plants. Additionally, *fitness* mutant shows high levels of *ProDH1* (*At3g30775*; Table S3) which was previously defined as a shared response gene of plants undergoing combined stress (Gupta & Senthil-Kumar, 2017).

3.5 | Altered expression of *FITNESS* promotes deregulation of ROS levels

The GO terms enrichment included several related to oxygen-containing compound and response to stress. Considering the importance of ROS as key signalling molecules involved in stress responses, we next detected the level of $O_2^{\cdot-}$ and H_2O_2 in *FITNESS* lines and WT Arabidopsis (Figures 4 and S4). Elevated levels of $O_2^{\cdot-}$ and H_2O_2 were present already in 20-day-old plants after overexpression of *FITNESS* (Figure S4). ROS accumulation in higher doses may lead to decreased growth and cell death finally affecting plant yield and productivity. To visualize cell death in *FITNESS* lines, trypan blue staining were performed. $FITNESS_{ox1}$ line showed higher trypan blue staining compatible with higher cell death when compared with control and *fitness-1* line (Figure S4).

We measured the antioxidant enzyme activities of SOD, CAT, APX, and GR in these lines. SOD and GR activities were elevated in $FITNESS_{ox}$ lines, meanwhile CAT and APX activities showed no difference with WT plants (Figures S5 and 4b). These data indicate that the enhanced antioxidant activities are not enough to efficiently scavenge ROS in $FITNESS_{ox}$ lines. In contrast, *fitness* mutants have significantly increased APX (Figure 4b) activity, whereas GR activity was decreased (Figure S5).

It is estimated that the majority of H_2O_2 in the cell is produced during photorespiration and photosynthesis (Foyer & Noctor, 2003; Kaurilind, Xu, & Brosché, 2015) making photorespiration an important contributor to cellular redox state. The incorporation of O_2 instead of CO_2 in the reaction catalysed by Rubisco produces 2-phosphoglycolate, which is irreversibly converted to glycolate and H_2O_2 by the enzyme glycolate oxidase (GOx) in the peroxisomes. The two genes encoding GOx that are coregulated with photorespiratory genes in Arabidopsis were analysed in our system. We found that 5-week-old *fitness* mutants have significantly lower transcript amount for both genes (*GOx1*, *At3g14415* and *GOx2*, *At3g14420*) leading to the thought that the photorespiratory pathway was less active in *fitness* plants. (Figure 4c,d). Expression of other genes related with photorespiration (Foyer, Bloom, Queval, & Noctor, 2009) was analysed in these lines in comparison with WT (Table S6). *fitness-1* mutants showed significantly reduced expression of genes encoding glycine decarboxylase subunits (*GLDP1*, *At4g33010* and *GLDP2*, *At2g26080*), chloroplast envelope transporters (*DIT1*, *At5g12860* and *DIT2.1*, *At5g64290*), CAT2 (*At4g35090*), and serine hydroxymethyltransferase (*SHM4*, *At4g13930*). Nevertheless, *fitness-1* mutants showed higher expression of genes encoding enzymes involved in the metabolic recycling of carbon and nitrogen such as glycerate kinase (*GLYK*, *At1g80380*), serine: glyoxylate aminotransferase (*SGAT2*, *At4g39660*) and glutamate dehydrogenase (*GDH*1, At5g18170 and *GDH*2, At5g07440). On the other hand, changes in the expression of genes involved in photorespiration were moderate in $FITNESS_{ox1}$ lines in comparison with WT plants. We also measured the levels of the metabolite glyoxylate in the leaves. $FITNESS_{ox}$ lines showed higher levels of glyoxylate (Figure S6), whereas in *fitness-1* mutants, glyoxylate content was similar to control levels. Photorespiratory pathway is intimately intertwined with plant metabolism (Kerchev et al., 2015), and changes in photorespiratory fluxes have an impact on plant metabolic network.

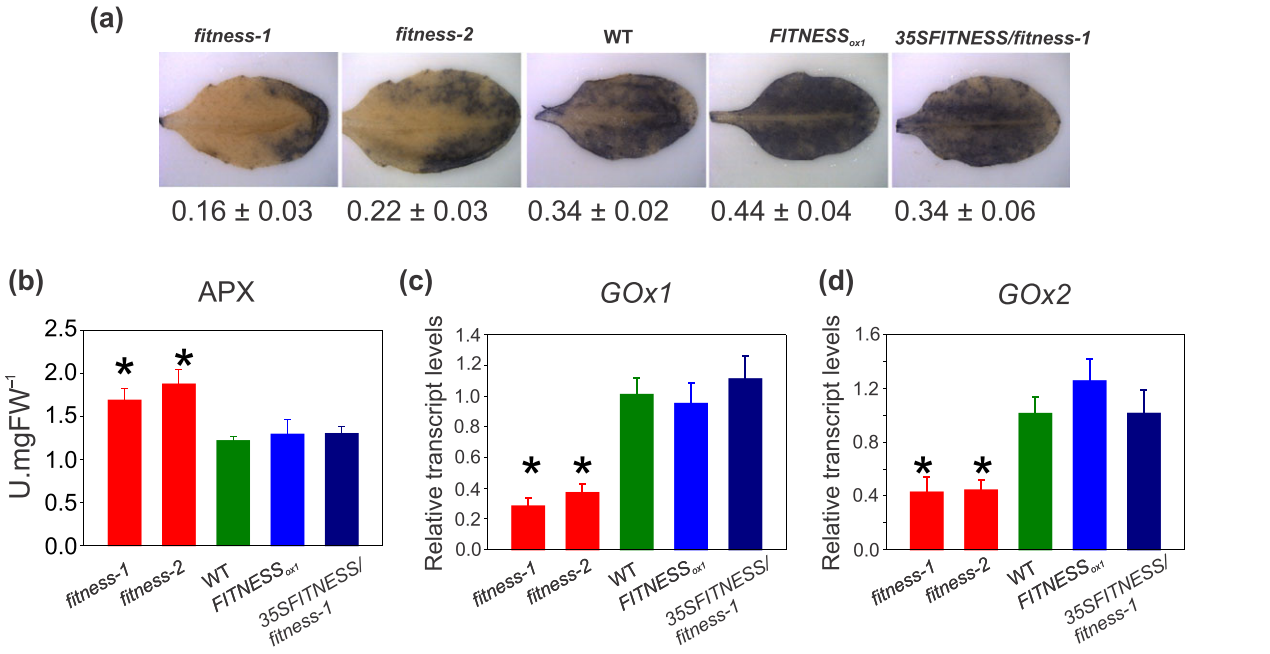

FIGURE 4 *FITNESS* deregulates endogenous reactive oxygen species levels. (a) NBT staining and quantification of *FITNESS* lines. Representative fully expanded rosette leaves of 3-week-old plants grown under long-day conditions were used. (b) Ascorbate peroxidase activities. (c) *GOx1* and (d) *GOx2* transcript levels were measured using qPCR in 5-week-old plants grown under normal growth conditions in long day. Both transcripts were significantly reduced in *fitness* mutants compared with WT. In (b, c, d), data are the means ± SE of three biological replicates. Statistical analyses were performed using the *t* test embedded in the Microsoft Excel software, statistically significant differences ($P < 0.05$) are indicated by *

3.6 | Metabolic changes related to altered ROS levels

In many plants, free Pro accumulates in response to stress operating not only as an osmoprotectant but also as a potent nonenzymatic antioxidant (Rejeb, Abdelly, & Savouré, 2014). As shown in Figure S6, free Pro accumulated in *FITNESS*$_{ox}$ lines of 5- and 6-week-old plants. At earlier stages, no differences in Pro was measured, but upon bolting, there was a steady increase in Pro levels suggesting a relationship between *FITNESS* expression, ROS levels, and Pro accumulation. The transcript levels of genes encoding Δ1-pyrroline-5-carboxylate synthetase1 (*P5CS1*, At2g39800) and Pro dehydrogenase 1 (*PDH1*, At3g30775) which are key enzymes in Pro synthesis and catabolism, respectively, were analysed. For *P5CS1*, higher and lower levels of transcripts were found in *FITNESS*$_{ox1}$ line and *fitness-1* mutant, respectively. However, for *PDH1*, only *fitness-1* mutant showed increased transcript levels (Table S7).

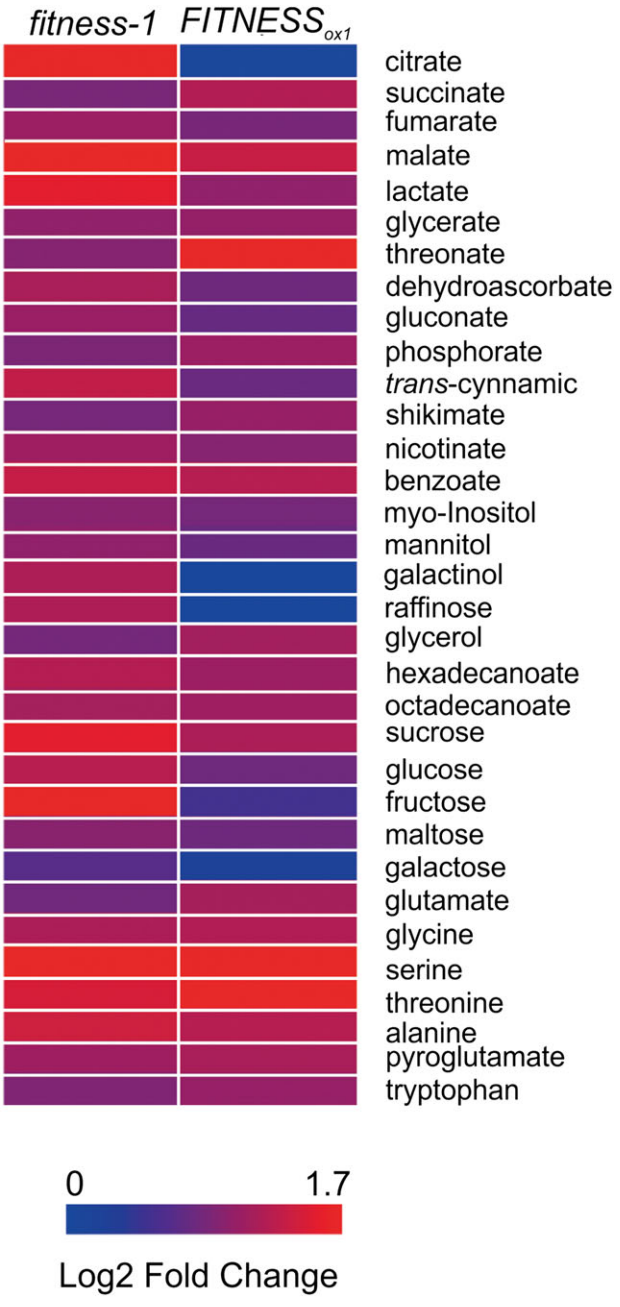

FIGURE 5 Heat map showing relative metabolite levels in *FITNESS* lines. Metabolite levels obtained using gas chromatography coupled to mass spectrometry in leaf extracts of 45-day-old plants grown under normal growth conditions in long day of *fitness-1* mutants, and *FITNESS*$_{ox1}$ line were calculated relative to WT and displayed as a heat map. Regions of red and blue indicate relative levels as depicted in the colour reference bar

Metabolic profiling by gas chromatography coupled to mass spectrometry was performed on extracts from rosette leaves of 45-day old of WT, *fitness-1*, and *FITNESS*$_{ox}$ lines plants. A total of 33 metabolites of known chemical structure were quantified in every chromatogram including amino acids, carbohydrates (sugars and sugar alcohols), and organic acids. Among the pool of the organic acids, *fitness-1* mutants accumulated higher levels of citrate, whereas it was not detected in *FITNESS*$_{ox}$ lines. Several sugars and sugar alcohols were differentially accumulated between the lines (Figure 5, Table S8). Of note, *FITNESS*$_{ox}$ lines showed drastic changes in galactinol and raffinose levels when compared with WT. Raffinose which belongs to the raffinose family oligosaccharides is a galactosyl–sucrose carbohydrate synthesized from galactinol and sucrose by the enzyme raffinose synthase. Both *fitness-1* mutants and *FITNESS*$_{ox1}$ line showed increased transcripts levels of genes encoding galactinol–sucrose galactosyl transferase 2 (*At3g57520*) and raffinose synthase (*At5g20250*). Galactinol synthesis involves the sugar galactose and the polyalcohol myo-inositol, and both were found decreased in *FITNESS*$_{ox}$ lines, reinforcing the finding of low levels of raffinose and galactinol. The expression of *galactinol synthase 1* (*At2g47180*) and *2* (*At1g56600*) in *fitness-1* mutants was significantly decreased. (Table S9).

Another change observed at the metabolic level was an increment of SA content in *fitness* mutants compared with WT (Figure 6a). In plants, there are two major pathways for SA synthesis, the isochorismate and the phenylalanine ammonia-lyase (PAL) pathways in which isochorismate synthase (ICS) and PAL are the critical enzymes, respectively. Both utilize chorismate, the end product of the shikimate pathway. Besides PAL contribution, the major route of SA biosynthesis is the IC pathway. Having observed an increment in SA, we analysed the transcript levels of the two genes encoding for ICS in Arabidopsis. *ICS1* transcripts were significantly increased in *fitness* mutants (Figure 6b) in agreement with earlier evidences showing that transcriptional control of *ICS1* is key for initiation of SA biosynthesis (Seyfferth & Tsuda, 2014). However, no increase in the *ICS2* transcript was observed in these lines (data not shown). SA accumulation is maintained through transcriptional regulation of *EDS1* (ENHANCED DISEASE SUSCEPTIBILITY 1; Du et al., 2009) and *PAD4* (PHYTOALEXIN DEFICIENT 4; Jirage et al., 1999) being both transcripts also upregulated in *fitness* mutants thereby contributing to SA accumulation (Figure 6c,d).

Rise of endogenous SA correlates with pathogenesis-related genes (*PR* genes) induction (Durrant & Dong, 2004). Transcriptional reprogramming is controlled mainly by nonexpressor of pathogenesis-related gene 1 (NPR1). Nuclear accumulation of NPR1 in the presence of SA results in *PR1* pathogenesis-related 1 (*PR1*) increased expression and is therefore considered a marker for activation of SA-signalling pathway. Consistent with the increased levels of SA measured in *fitness* mutants, we observed an induction of both *NPR1*

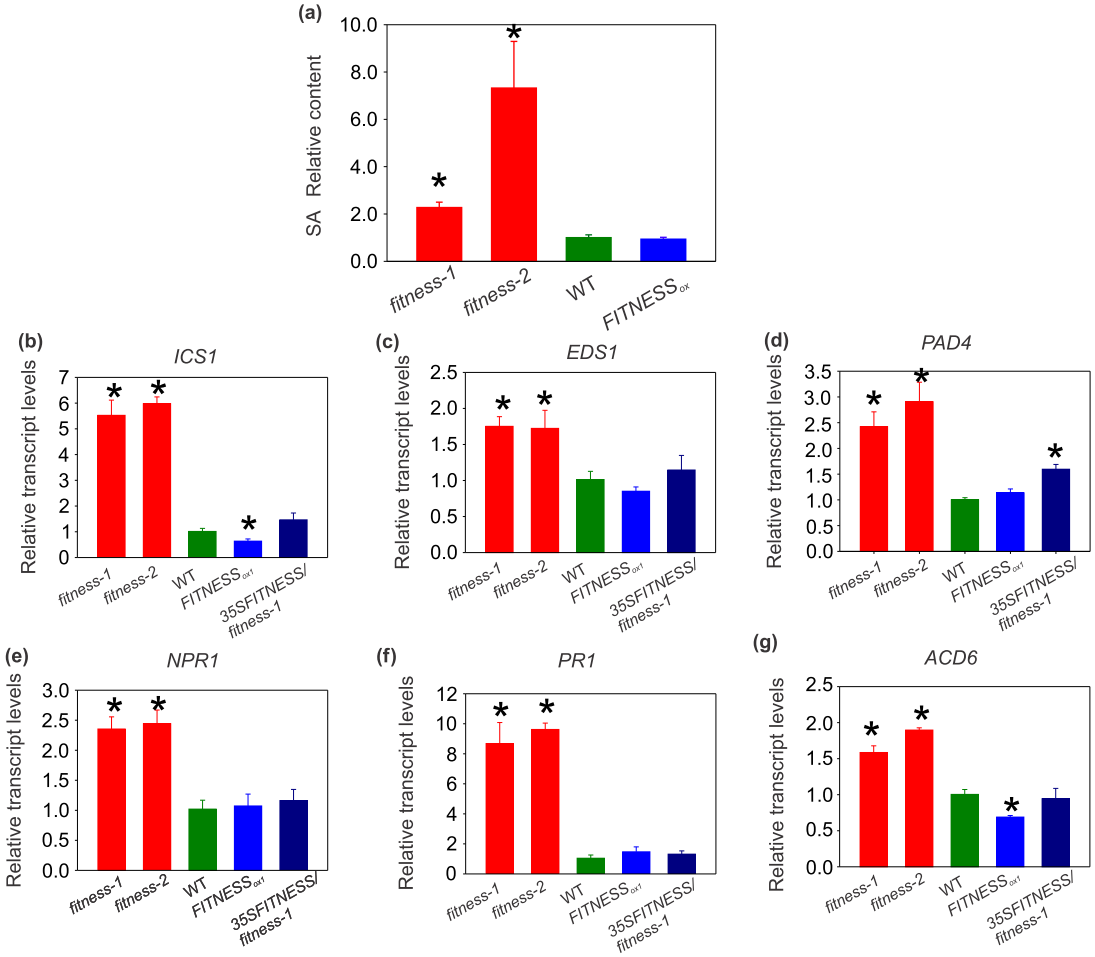

FIGURE 6 FITNESS leads to changes in salicylic acid (SA) levels. (a) Salicylic acid was measured using gas chromatography coupled to mass spectrometry, and its relative concentration was determined by comparison with WT values including the internal standard ribitol. Methanolic extract were prepared from 5-week-old plants grown under normal growth conditions in long day. (b) *ICS1*, (c) *EDS1*, (d) *PAD4*, (e) *NPR1*, (f) *PR1*, (g) *ACD6* transcript levels measured using qPCR in 5-week-old plants grown under normal growth conditions. Data are the means ± SE of three biological replicates. Statistical analyses were performed using the *t* test embedded in the Microsoft Excel software, statistically significant differences ($P < 0.05$) are indicated by *

and *PR1* transcript levels (Figure 6e,f). As SA is required for *ACD6* function (Lu, Rate, Song, & Greenberg, 2003), we also analysed its transcript levels, and we could confirm that *fitness* mutants show increased transcripts levels for this gene (Figure 6g).

3.7 | Enhanced oxidative stress tolerance of *fitness* mutants

To investigate the tolerance of *FITNESS* lines towards MV, which generates $O_2^{\cdot-}$ in the chloroplast during photosynthesis, 3-week-old plants were sprayed with MV (15 μM in 0.1% Tween-20). Plants sprayed with the same solution but without MV were taken as control. After 16-hr treatment, significantly higher chlorophyll *a* content as well lower electrolyte leakage was measured in both *fitness* mutants (Figure 7a(left),b,c). When a stronger treatment using 50 μM MV was used in 4-week-old plants, leaves showed visible symptoms of bleaching, but at 12 days after treatment, *fitness* mutants resumed growth, and green rosette leaves were visible indicating tolerance against MV (Figure 7a right panel). On the contrary, in WT plants and $FITNESS_{ox}$ lines, MV treatment resulted in plant death, suggesting that *FITNESS* is involved in oxidative stress tolerance in Arabidopsis. This idea is in agreement with the lower level of ROS detected in *fitness* mutants after 2 hr 50 μM MV treatment (Figure 7d).

It was reported that JUB1, a NAC transcription factor, is rapidly and strongly induced by H_2O_2 (Wu et al., 2012). JUB1 participates in regulating the cellular H_2O_2 homeostasis network and constitutes a central regulator of cellular H_2O_2 level. Additionally, *JUB1* expression in leaves increases towards the tip (Wu et al., 2012) opposite to *FITNESS* promoter activity which decreases toward the tip of the leaf (Figure 7e) indicating that FITNESS could act as a negative regulator of JUB1. Taking this into account, we decided to measure *JUB1* transcript levels in *FITNESS* lines. *fitness* mutants showed a strong upregulation of *JUB1* in leaves (Figure 7f). Altogether, these data support the idea that *FITNESS* acts upstream *JUB1* thereby controlling H_2O_2 levels.

4 | DISCUSSION

Several studies have demonstrated that ROS control diverse processes in plants such as growth and development, stress response, pathogen

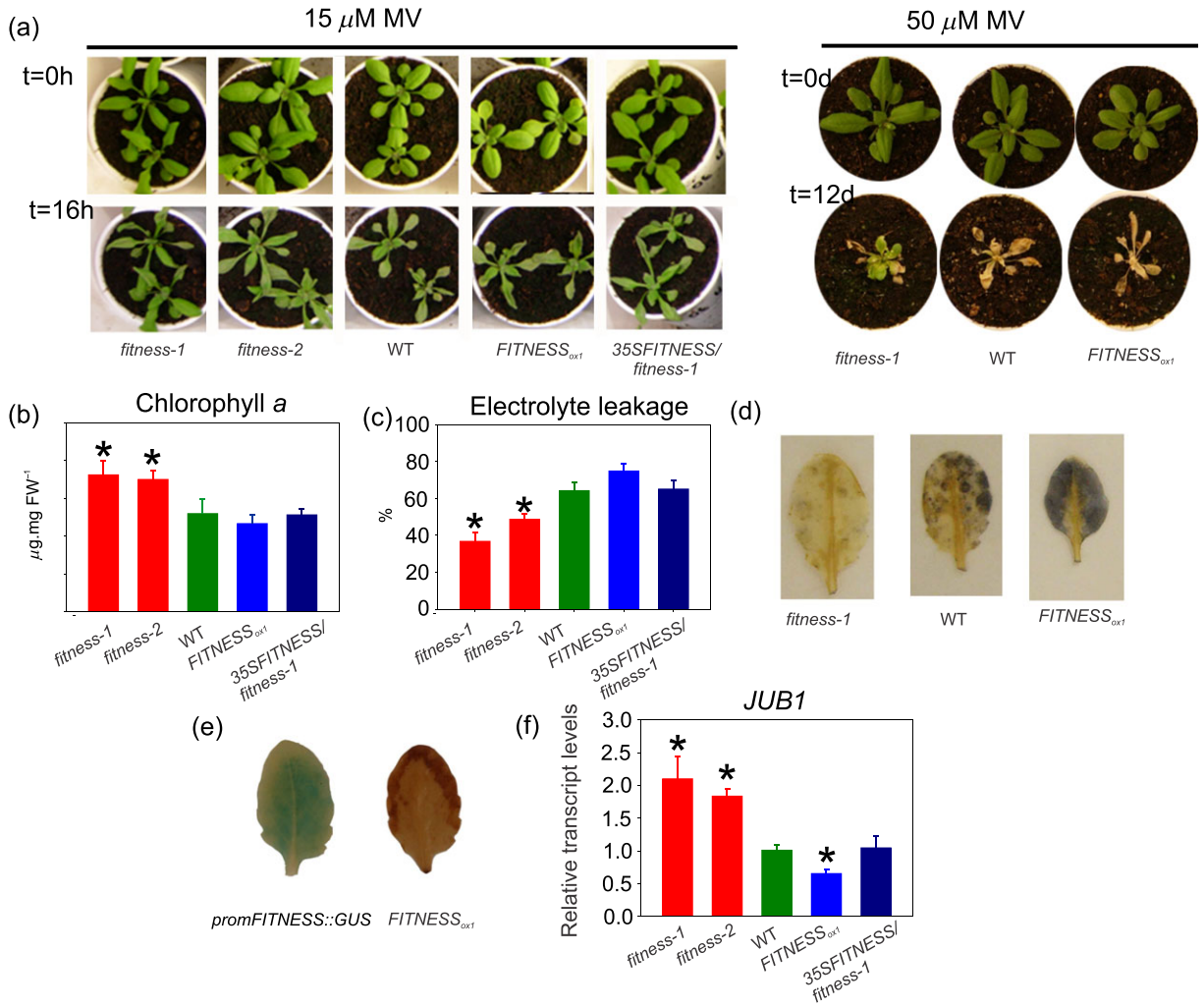

FIGURE 7 *FITNESS* lines show altered tolerance to oxidative stress and altered *JUB1* expression. (a) Three- (left panel) and four- (right panel) week-old plants grown under normal growth conditions were sprayed with methyl viologen (MV; 15 and 50 μM in 0.1% Tween-20, respectively) and exposed to light. Representative results are presented. *fitness* mutants resulted more tolerant to MV treatment as a result of a better reactive oxygen species detoxification. (b) Chlorophyll *a* level and (c) Electrolyte leakage after 16 hr 15 μM MV treatment of *FITNESS* lines. (d) NBT staining revealed lower superoxide anion levels in *fitness* mutants after 2 hr 50 μM MV treatment (right panel) (e) GUS expression and reactive oxygen species levels show an opposite pattern of accumulation. Left panel: GUS staining of a 4-week fully developed *promFITNESS::GUS* leaf showing decreased *FITNESS* expression towards the tip of the leaf. The right panel shows a representative leaf of $FITNESS_{ox}$ line showing accumulation of H_2O_2 in the border of the leaf visualized with DAB staining. (f) *JUB1* expression levels were determined by qPCR in 5-week-old plants grown under normal growth conditions in long day. Error bars represent the means ± SE of three biological replicates. Statistical analyses were performed using the *t* test embedded in the Microsoft Excel software, statistically significant differences ($P < 0.05$) are indicated by *

defence, and hormonal signalling (Davletova et al., 2005). In our attempt to understand the role of FITNESS in Arabidopsis, we observed that its altered expression leads to deregulation of ROS levels. Specifically, high ROS levels were accompanied with stunted growth and delay in flowering time in $FITNESS_{ox}$ lines. *FITNESS* overexpression leads to reduced seed yield contrary to *fitness* mutants which showed higher seed yield. Crops producing higher seed yield is one of the big challenges nowadays. During the daylight period, plants need to accurately control redox homeostasis to prevent ROS overload due to excess light. In higher plants, photoprotection is achieved through thermal dissipation of excess light energy. $FITNESS_{ox}$ lines have increased NPQ which is the most important short-term reversible photoprotective process in higher plants. However, chronic high NPQ provokes a significant cost because CO_2 assimilation per unit of absorbed light is decreased.

Multiple molecular mechanisms converge to alter core cellular metabolism. Failure to maintain redox balance results in growth defects or initiation of plant cell death. $FITNESS_{ox}$ plants cultivated in controlled environment growth chambers show decreased growth relative to WT, accumulate ROS, and show altered levels of metabolites and transcripts of enzymes involved in photorespiration.

Photorespiration lowers photosynthetic efficiency due to CO_2 and ammonia loss and consumption of ATP and reducing power in their reassimilation pathways. Maurino and Weber (2013) speculated that a reduction of photorespiration rate should enhance CO_2 fixation and plant growth. In this context, we postulate that *fitness* mutant

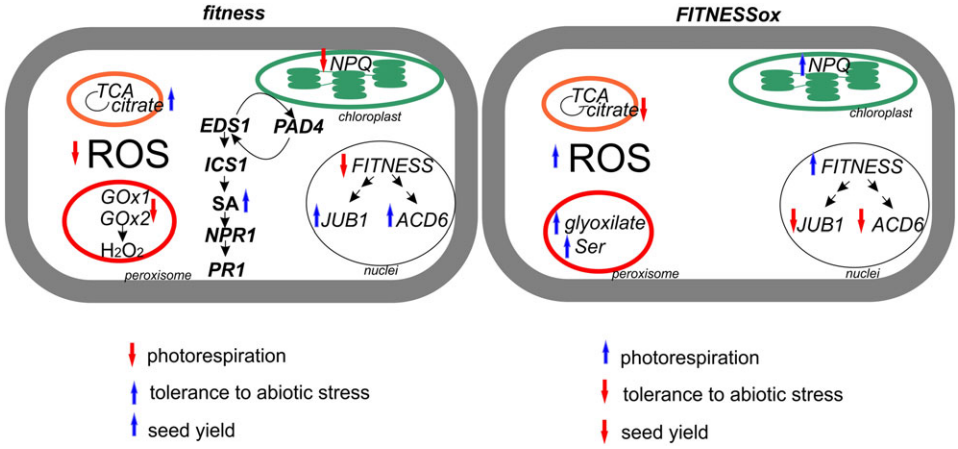

FIGURE 8 Schematic action of *FITNESS*. ROS: reactive oxygen species; GO: Gene Ontology; NPQ: nonphotochemical quenching

phenotype is directly related with the better photosynthetic performance of these plants. Here, we demonstrate that a single gene is able to modify photorespiratory metabolites and transcripts leading to increased seed yield. Accumulation of glyoxylate can directly lead to a feedback regulation of photosynthetic activity through regulation of Rubisco activation state (Häusler et al., 1996), therefore glyoxylate can be seen as an in vivo photosynthesis feedback inhibitor. Moreover, recently GOx was found to physically interact with CAT leading thereby to reversible adjustment of H_2O_2 levels (Z. Zhang et al., 2016). Dissociation of GOx–CAT complex induces an increase in cellular H_2O_2 which acts as a signal to regulate physiological processes.

Low levels of citrate in *FITNESS*$_{ox}$ lines indicate a break in the tricarboxylic acid cycle. Pyruvate dehydrogenase complex links glycolysis and oxidative catabolism of sugars by irreversible decarboxylation of pyruvate to acetyl-CoA which in turns is fused to oxalacetate, catalysed by citrate synthase. The formation of acetyl CoA is a highly regulated step and is inhibited when ATP and NAD (P) H are formed in mitochondria as products of photorespiration leading to citrate depletion (Bauwe, Hagemann, & Fernie, 2010).

Pro, on the other hand, was high in *FITNESS*$_{ox}$ lines, in agreement with transcript levels of both key enzymes involved in Pro metabolism. It was previously reported that endogenous H_2O_2 concentration rises during bolting in Arabidopsis leaves and down-regulation of CAT2 activity was suggested to be the initial step of this rise (Zimmermann, Heinlein, Orendi, & Zentgraf, 2006). The rise in Pro level overlaps ROS accumulation in *FITNESS*$_{ox}$ lines. Pro has a unique role in stress adaptation. Multiple and complex regulatory pathways can alter Pro metabolism under stress (L. Zhang & Becker, 2015), and its metabolism has been proposed as a helper in keeping the NADPH/$NADP^+$ balance and GSH levels (Liang, Zhang, Natarajan, & Becker, 2013). Taking into account that Pro can act as a potent nonenzymatic antioxidant (Rejeb et al., 2014), its accumulation along with ROS rise in *FITNESS*$_{ox}$ lines may contribute to partially alleviate the oxidative damage in these plants.

FITNESS$_{ox}$ lines showed low raffinose and galactinol levels. Their intracellular accumulation in plant cells is closely associated with environmental stress responses (ElSayed, Rafudeen, & Golldack, 2013), and it has been proposed that one of the main roles of these oligosaccharides is to scavenge ROS in the cytosol and in the chloroplast (Nishiawa, Yabuta, & Shigeoka, 2008). As *FITNESS*$_{ox}$ lines accumulate high level of ROS, the measured low levels of galactinol and raffinose might contribute to the scavenging failure and spontaneous lesion formation on the leaves, or alternatively, they were depleted due to the high ROS level in *FITNESS*$_{ox}$ lines.

H_2O_2 is not only a by-product of photorespiration but also a regulator of plant cell death. Lesion formation in *FITNESS*$_{ox}$ lines can be regarded as a consequence of ROS accumulation. Peroxisomal H_2O_2 is also able to trigger SA-related responses in tobacco and to activate the ICS-dependent SA synthesis pathway in Arabidopsis (Z. Zhang et al., 2016). Notably, *fitness* mutants accumulate higher amounts of SA, which correlates with *ICS1* transcript up-regulation. Expression profiling of mutants impacted in SA hormone pathway has placed *PAD4* and *EDS1* upstream of *ICS1*. EDS1 and PAD4 participate in a defence amplification loop that responds to SA and ROS intermediates (Rusterucci et al., 2001). The finding that *PAD4* and *EDS1* transcripts are both up-regulated in *fitness* mutants confirms that this ROS perturbation leads to modification of hormonal homeostasis. Wituszynska et al. (2013) have reported that LSD1, EDS1, and PAD4 play important roles in plant fitness regulation and seed yield, which is in agreement with our results. Our data indicate that altered expression of *FITNESS* acts modulating SA-related processes. Noteworthy, reproductive success is not compromised although a high level of expression of defence responses related genes is present in *fitness* mutants, similarly to Arabidopsis accession C24 which achieves constitutive expression of pathogen defences and drought tolerance without incurring a yield penalty (Bechtold et al., 2010) and Arabidopsis *cdd1* mutant that accumulates high level of SA but maintains a normal growth (Swain, Singh, & Nandi, 2015). Indeed, *ACD6*, and two defence-related genes *PCC1* and *LURP1*, showed increased expression in *fitness* mutants, *ACD6* encodes a transmembrane protein which acts in a feed-forward loop that regulates the accumulation of SA and induces *PR1* transcripts increased levels (Lu et al., 2003). Similarly to *FITNESS*$_{ox}$ lines, *acd6-1* plants have necrotic lesions. Additionally, it was postulated that altered *ACD6* activity has additive effects on total biomass (Todesco et al., 2010). *fitness* mutants show also high transcriptional up-regulation of the SA-responsive marker gene *PR1*, whose expression is NPR1-dependent. Additionally, NPR1 translocation to the nucleus in its active monomeric form is redox dependent and mediated by SA.

These evidences suggest that a fine-tuning regulation is exerted by SA. On one hand, SA can promote ROS production which are essential for defence responses; on the other hand, SA promotes ROS scavenging being essential for antioxidant responses as in high light, avirulent bacteria and salinity (Rivas-San Vicente & Plasencia, 2011).

It was postulated that JUB1 constitutes a central regulator in the cellular H_2O_2 level, and it primes plants for upcoming stress through a gene regulatory network (Wu et al., 2012). A strong tolerance to chloroplast oxidative stress was found in *fitness* mutants, contrary to $FITNESS_{ox}$ lines (Figure 7). In *fitness* and $FITNESS_{ox}$ plants, *JUB1* expression was highly up- and down-regulated, respectively. These data suggest that *FITNESS* negatively regulates *JUB1* expression by acting upstream JUB1 in the environmental stress regulatory pathway. When FITNESS is absent, *JUB1* expression increases, and plants are better prepared to overcome oxidative stress as it was observed in *fitness* plants.

A summary of present data is shown in Figure 8. At early stage of ROS generation in the chloroplast during photosynthesis, *FITNESS* transcripts are strongly downregulated as a rapid antioxidant response of the plant (Scarpeci et al., 2008). To mimic this situation permanently, FITNESS levels were dramatically diminished in Arabidopsis plants during the whole life cycle (*fitness* mutant). A great advantage to the plant was observed, lowering photorespiratory metabolites and transcripts, decreasing ROS levels, decreasing NPQ, and increasing SA and thereby SA-responsive genes. Consequently and because there is no need to detoxify ROS, the antioxidant response is lowered, and plant performance is optimized leading to high seed yield. In the opposite situation, if FITNESS level is permanently present in the cell, increased photorespiratory metabolites and transcripts and very high ROS levels are produced, and they cannot be scavenged in spite of increased antioxidant activities resulting in cell death.

ACKNOWLEDGEMENTS

This research funding was provided by ANPCYT and CONICET from Argentina. D. A. M. was awarded a Jeff Schell Fellowship from Bayer Science & Education Foundation to perform experiments at the MPI-MP.

ORCID

Salma Balazadeh http://orcid.org/0000-0002-5789-4071
María Inés Zanor http://orcid.org/0000-0002-8903-0673

REFERENCES

Anders, S., & Huber, W. (2010). Differential expression analysis for sequence count data. *Genome Biology*, *11*, R106.

Baker, N. R., & Rosenqvist, E. (2004). Applications of chlorophyll fluorescence can improve crop production strategies: An examination of future possibilities. *Journal of Experimental Botany*, *55*, 1607–1621.

Bauwe, H., Hagemann, M., & Fernie, A. R. (2010). Photorespiration: Players, partners and origin. *Trends in Plant Science*, *15*, 330–336.

Baxter, A., Mittler, R., & Suzuki, N. (2013). ROS as key players in plant stress signaling. *Journal of Experimental Botany*, *65*, 1229–1240.

Beauchamp, C., & Fridovich, I. (1971). Superoxide dismutase: Improved assays and an assay applicable to acrylamide gels. *Analytical Biochemistry*, *44*, 276–287.

Bechtold, U., Lawson, T., Mejia-Carranza, J., Meyer, R. C., Borwn, I. R., Altmann, T., … Mullineaux, P. M. (2010). Constitutive salicylic acid defenses do not compromise seed yield, drought tolerance and water productivity in the Arabidopsis accession C24. *Plant, Cell & Environment*, *33*, 1959–1973.

Bournonville, C. F., & Díaz-Ricci, J. C. (2011). Quantitative determination of superoxide in plant leaves using a modified NBT staining method. *Phytochemical Analalysis*, *22*, 268–271.

Cockram, J., Thiel, T., Steuernagel, B., Stein, N., Taudien, S., Bailey, P., & O'Sullivan, D. M. (2012). Genome dynamics explain the evolution of flowering time CCT domain gene families in the Poaceae. *PLoS One*, *7*, e45307. https://doi.org/10.1371/journal.pone.0045307

Czechowski, T., Stitt, M., Altmann, T., Udvardi, M. K., & Scheible, W. R. (2005). Genome-wide identification and testing of superior reference genes for transcript normalization in Arabidopsis. *Plant Physiology*, *139*, 5–17.

Davletova, S., Rizhsky, L., Shenggiang, Z., Oliver, D. J., Coutu, J., Shulaev, V., … Mittler, R. (2005). Cytosolic ascorbate peroxidase 1 is a central component of the reactive oxygen network of Arabidopsis. *Plant Cell*, *17*, 268–281.

Di Rienzo, J. A., Casanoves, F., Balzarini, M. G., Gonzalez, L., Tablada, M., & Robledo, C. W. (2008). In Grupo InfoStat, FCA (Ed.), *InfoStat*, *versión 2008*. Argentina: Universidad Nacional de Córdoba.

Du, L., Ali, G. S., Simons, K. A., Hou, J., Yang, T., & Reddy, A. S. (2009). Ca^{2+}/calmodulin regulates salicylic-acid-mediated plant immunity. *Nature*, *457*, 1154–1158.

Durrant, W. E., & Dong, X. (2004). Systemic acquired resistance. *Annual Review of Phytopathology*, *42*, 185–209.

ElSayed, A. I., Rafudeen, M. S., & Golldack, D. (2013). Physiological aspects of raffinose family oligosaccharides in plants: Protection against abiotic stress. *Plant Biology*, *16*, 1–8.

Foyer, C. H., Bloom, A. J., Queval, G., & Noctor, G. (2009). Photorespiratory metabolism: Genes, mutants, energetics and redox signaling. *Annual Review of Plant Biology*, *60*, 455–484.

Foyer C.H. **&,** Noctor G. (2003) Redox sensing and signalling associated with reactive oxygen in chloroplasts, peroxisomes and mitochondria. *Physiologia Plantarum 119*, 355–364

Gendron, J. M., Pruneda-Paz, J. L., Doherty, C. J., Gross, A. M., Kang, S. E., & Kay, S. A. (2012). Arabidopsis circadian clock protein, TOC1, is a DNA-binding transcription factor. *Proceedings of the National Academy of Sciences, USA*, *109*, 3167–3172.

Gupta, A., & Senthil-Kumar, M. (2017). Transcriptome changes in Arabidopsis thaliana infected with Pseudomonas syringae during drought recovery. *Scientific Reports*, *7*, 9124. https://doi.org/10.1038/s41598-017-09135-y

Häusler, R. E., Bailey, K. J., Lea, P. J., & Leegood, R. C. (1996). Control of photosynthesis in barley mutants with reduced activities of glutamine synthetase and glutamate synthase. *Planta*, *200*, 388–396.

Horton, P., Park, K. J., Obayashi, T., Fujita, N., Harada, H., Adams-Collier, C. J., & Nakai, K. (2007). WolF PSORT: Protein localization predictor. *Nucleic Acids Research*, *35*, W585–W587.

Hyun, Y., Cho, S. W., Choi, Y., Kim, J. S., & Coupland, G. (2015). Site-directed mutagenesis in Arabidopsis thaliana using dividing tissue-targeted RGEN of the CRISPR/Cas system to generate heritable null alleles. *Planta*, *241*, 271–284.

Jarvis, P., Chen, L. J., Li, H., Peto, C. A., Fankhauser, C., & Chory, J. (1998). An Arabidopsis mutant defective in the plastid general protein import apparatus. *Science*, *282*, 100–103.

Jirage, D., Tootle, T. L., Reuber, L., Frost, L. N., Feys, B. J., Parker, J. E., … Glazebrook, J. (1999). Arabidopsis thaliana PAD4 encodes a lipase-like gene that is important for salicylic acid signaling. *Proceedings of the National Academy of Sciences, USA 96*, 13583–13588.

Kaczorowski, K. A., & Quail, P. H. (2003). Arabidopsis PSEUDO-RESPONSE REGULATOR7 is a signaling intermediate in phytochrome-regulated seedling deetiolation and phasing of the circadian clock. *Plant Cell*, *15*, 2654–2665.

Kaurilind, E., Xu, E., & Brosché, M. (2015). A genetic framework for H_2O_2 induced cell death in *Arabidopsis thaliana*. *BMC Genomics 16*, 837.

Kerchev, P., Mühlenbock, P., Denecker, J., Morreel, K., Hoeberichts, F. A., Van Der Kelen, K., & Van Breusegem, F. (2015). Activation of auxin signaling counteracts photorespiratory H_2O_2-dependent cell death. *Plant Cell & Environment*, *38*, 253–265.

Kim, D., Langmead, B., & Salzberg, S. L. (2015). HISAT: A fast spliced aligner with low memory requirements. *Nature Methods*, *12*, 357–360.

Kosugi, S., Hasebe, M., Matsamura, N., Takashima, H., Miyamoto-Sato, E., Tomita, M., & Yanagawa, H. (2009). Six classes of nuclear localization signals specific to different binding grooves of importin α. *Journal of Biological Chemistry*, *284*, 478–485.

Larkin, M. A., Blackshields, G., Brown, N. P., Chenna, R., McGettigan, P. A., McWilliam, H., & Higgins, D. G. (2007). Clustal W and Clustal X version 2.0. *Bioinformatics*, *23*, 2947–2948.

Liang, X., Zhang, L., Natarajan, S. K., & Becker, D. F. (2013). Proline mechanisms of stress survival. *Antioxidants & Redox Signaling*, *19*, 998–1011.

Lisec, J., Schauer, N., Kopka, J., Willmitzer, L., & Fernie, A. R. (2006). Gas chromatography mass spectrometry-based metabolite profiling in plants. *Nature Protocols*, *1*, 387–396.

Lu, H., Rate, D. N., Song, J. T., & Greenberg, J. T. (2003). ACD6, a novel ankyrin protein, is a regulator and an effector of salicylic acid signaling in the Arabidopsis defense response. *Plant Cell*, *15*, 2408–2420.

Maurino, V. G., & Weber, A. P. M. (2013). Engineering photosynthesis in plants and synthetic microorganisms. *Journal of Experimental Botany*, *64*, 743–751.

Michelet, L., & Krieger-Liszkay, A. (2012). Reactive oxygen intermediates produced by photosynthetic electron transport are enhanced in short-day grown plants. *Biochimica et Biophysica Acta*, *1817*, 1306–1313.

Mittler, R., Vanderauwera, S., Gollery, M., & Van Breusegem, F. (2004). Reactive oxygen gene network of plants. *Trends in Plant Science*, *9*, 490–498.

Mulki, M. A., & von Korff, M. (2016). CONSTANS controls floral repression by up-regulating VERNALIZATION2 (VRN-H2) in barley. *Plant Physiology*, *170*, 325–337.

Nishiawa, A., Yabuta, Y., & Shigeoka, S. (2008). Galactinol and raffinose constitute a novel function to protect plants from oxidative damage. *Plant Physiology*, *147*, 1251–1263.

Ordoñez Herrera, N., Trimborn, L., Menje, M., Henschel, M., Robers, L., Kaufholdt, D., … Hoecker, U. (2018). The transcription factor COL12 is a substrate of the COP1/SPA E3 ligase and regulates flowering time and plant architecture. *Plant Physiology*, *176*, 1327–1340.

Page, R. D. M. (1996). TREEVIEW: An application to display phylogenetic trees on personal computers. *Bioinformatics*, *12*, 357–358.

Pertea, M., Kim, D., Pertea, G. M., Leek, J. T., & Salzberg, S. L. (2016). Transcript-level expression analysis of RNA-seq experiments with HISAT, StringTie and Ballgown. *Nature Protocols*, *11*, 1650–1667.

Pfaffl, M. W. (2001). A new mathematical model for relative quantification in real-time RT-PCR. *Nucleic Acids Research*, *29*, e45–e445.

Puterill, J., Robson, F., Lee, K., Simon, R., & Coupland, G. (1995). The CONSTANS gene of Arabidopsis promotes flowering and encodes a protein showing similarities to zinc finger transcription factors. *Cell*, *24*, 847–857.

Queval, G., Issakidis-Bourguet, E., Hoeberichts, F. A., Vandorpe, M., Gakière, B., Vanacker, H., & Noctor, G. (2007). Conditional oxidative stress responses in the Arabidopsis photorespiratory mutant cat2 demonstrate that redox state is a key modulator of daylength-dependent gene expression, and define photoperiod as a crucial factor in the regulation of H_2O_2-induced cell death. *Plant Journal*, *52*, 640–657.

Rejeb, K. B., Abdelly, C., & Savouré, A. (2014). How reactive oxygen species and proline face stress together. *Plant Physiology and Biochemistry*, *80*, 278–284.

Rivas-San Vicente, M., & Plasencia, J. (2011). Salicylic acid beyond defense: Its role in plant growth and development. *Journal of Experimental Botany*, *62*, 3321–3338.

Rusterucci, C., Aviv, D. H., Holt, III, B. F., Dangl, J. L., & Parker, J. E. (2001). The disease resistance signaling components EDS1 and PAD4 are essential regulators of the cell death pathway controlled by LSD1 in Arabidopsis. *Plant Cell*, *13*, 2211–2224.

Rutledge, R. G., & Stewart, D. (2008). A kinetic-based sigmoidal model for the polymerase chain reaction and its application to high-capacity absolute quantitative real-time PCR. *BMC Biotechnology*, *8*, 47.

Scarpeci, T., Zanor, M. I., Mueller-Roeber, B., & Valle, E. (2013). Overexpression of AtWRKY30 enhances abiotic stress tolerance during early growth stages in Arabidopsis thaliana. *Plant Molecular Biology*, *83*, 265–277.

Scarpeci, T. E., Frea, V., Zanor, M. I., & Valle, E. M. (2017). Overexpression of AtERF019 delays plant growth and senescence, and improves drought tolerance in Arabidopsis. *Journal of Experimental Botany*, *68*, 673–685.

Scarpeci, T. E., Zanor, M. I., Carrillo, N., Mueller-Roeber, B., & Valle, E. M. (2008). Generation of superoxide anion in chloroplasts of *Arabidopsis thaliana* during active photosynthesis: A focus on rapidly induced genes. *Plant Molecular Biology*, *66*, 361–378.

Schauer, N., Steinhauser, D., Strelkov, S., Schomburg, D., Allison, G., Moritz, T., & Kopka, J. (2005). GCMS libraries for the rapid identification of metabolites in complex biological samples. *FEBS Letters*, *579*, 1332–1337.

Seyfferth, C., & Tsuda, K. (2014). Salicylic acid signal transduction: The initiation of biosynthesis, perception and transcriptional reprogramming. *Frontiers in Plant Science*, *5*, 697. https://doi.org/10.3389/fpls.2014.00697

Strayer, C., Oyama, T., Schiultz, T. F., Raman, R., Somers, D. E., Más, P., … Kay, S. A. (2000). Cloning of the Arabidopsis clock gene TOC1, an autoregulatory response regulator homolog. *Science*, *289*, 768–771.

Sun, C., Huang, Y., & Chang, H. (2009). CIA_2 coordinately up-regulates protein import and synthesis in leaf chloroplasts. *Plant Physiology*, *150*, 879–888.

Swain, S., Singh, N., & Nandi, A. K. (2015). Identification of plant defence regulators through transcriptional profiling of Arabidopsis thaliana cdd1mutant. *Journal of Biosciences*, *40*, 1–10.

Tian, T., Liu, Y., Yan, H., You, Q., Yi, X., Du, Z., … Su, Z. (2017). agriGO v2.0: A GO analysis toolkit for the agricultural community. *Nucleic Acids Research* gkx382. doi: https://doi.org/10.1093/nar/gkx382, *45*, W122–W129.

Tiwari, S. B., Shen, Y., Chang, H. C., Hou, Y., Harris, A., Ma, S. F., & Ratcliffe, O. J. (2010). The flowering time regulator CONSTANS is recruited to the FLOWERING LOCUS T promoter via a unique *cis*-element. *New Phytologist*, *187*, 57–66.

Todesco, M., Balasubramanian, S., Hu, T. T., Traw, M. B., Horton, M., Epple, P., … Weigel, D. (2010). Natural allelic variation underlying a major fitness trade-off in Arabidopsis thaliana. *Nature*, *465*, 632–636.

Wituszynska, W., Slesak, I., Vanderauwera, S., Szechynka-Hebda, M., Kornas, A., Van Der Kelen, K., & Karpinski, S. (2013). LESION SIMULATING DISEASE1, ENHANCED DISEASE SUSCEPTIBILITY1, and PHYTOALEXIN DEFICIENT4 conditionally regulate cellular signaling homeostasis, photosynthesis, water use efficiency, and seed yield in Arabidopsis. *Plant Physiology*, *161*, 1795–1805.

Wu, A., Allu, A. D., Garapati, P., Siddiqui, H., Dortay, H., Zanor, M. I., & Balazadeh, S. (2012). JUNGBRUNNEN1, a reactive oxygen species-responsive NAC transcription factor, regulates longevity in Arabidopsis. *Plant Cell*, *24*, 82–506.

Yano, M., Katayose, Y., Ashikari, M., Yamanouchi, U., Monna, L., Fuse, T., … Sasaki, T. (2000). *Hd1*, a major photoperiod sensitivity quantitative trait locus in rice, is closely related to the Arabidopsis flowering time gene CONSTANS. *Plant Cell*, *12*, 2473–2484.

Zhang, L., & Becker, D. (2015). Connecting proline metabolism and signaling pathways in plant senescence. *Frontiers in Plant Science*, *6*, 552.

Zhang, Z., Xu, Y., Xie, Z., Li, X., He, Z., & Peng, X. (2016). Association-dissociation of glycolate oxidase with catalase in rice: A potential switch to modulate intracellular H_2O_2 levels. *Molecular Plant*, *9*, 737–748.

Zimmermann, P., Heinlein, C., Orendi, G., & Zentgraf, U. (2006). Senescence-specific regulation of catalases in *Arabidopsis thaliana* (L.) Heynh. *Plant, Cell & Environment*, *29*, 1049–1060.

SUPPORTING INFORMATION

Additional supporting information may be found online in the Supporting Information section at the end of the article.

How to cite this article: Osella AV, Mengarelli DA, Mateos J, et al. FITNESS, a CCT domain-containing protein, deregulates reactive oxygen species levels and leads to fine-tuning trade-offs between reproductive success and defence responses in Arabidopsis. *Plant Cell Environ*. 2018;41:2328–2341. https://doi.org/10.1111/pce.13354